Published in final edited form as:
Biomaterials. 2011 December ; 32(36): 9677–9684. doi:10.1016/j.biomaterials.2011.08.084.

Extrahepatic islet transplantation with microporous polymer scaffolds in syngeneic mouse and allogeneic porcine models

Romie F. Gibly[a,b], **Xiaomin Zhang**[c], **Melanie L. Graham**[d,e], **Bernhard J. Hering**[d,e], **Dixon B. Kaufman**[f], **William L. Lowe Jr**[g], and **Lonnie D. Shea**[a,h,i,j,*]

[a]Institute of Bionanotechnology in Medicine (IBNAM), Northwestern University, Chicago, IL, 60611, USA

[b]Integrated Graduate Program, Northwestern University, Chicago, IL, 60611, USA

[c]Department of Surgery, Northwestern University, Chicago, IL, 60611, USA

[d]Department of Surgery, University of Minnesota, Minneapolis, MN, 55455, USA

[e]Schulze Diabetes Institute, University of Minnesota, Minneapolis, MN, 55455, USA

[f]Department of Surgery, University of Wisconsin, Madison, WI, 53792, USA

[g]Department of Medicine, Northwestern University, Chicago, IL, 60611, USA

[h]Department of Chemical and Biological Engineering, Northwestern University, Evanston, IL, 60208, USA

[i]Chemistry of Life Processes Institute, Northwestern University, Evanston, IL, 60208, USA

[j]The Robert H. Lurie Comprehensive Cancer Center of Northwestern University, Chicago, IL, 60611, USA

Abstract

Intraportal transplantation of islets has successfully treated select patients with type 1 diabetes. However, intravascular infusion and the intrahepatic site contribute to significant early and late islet loss, yet a clinical alternative has remained elusive. We investigated non-encapsulating, porous, biodegradable polymer scaffolds as a vehicle for islet transplantation into extrahepatic sites, using syngeneic mouse and allogeneic porcine models. Scaffold architecture was modified to enhance cell infiltration leading to re-vascularization of the islets with minimal inflammatory response. In the diabetic mouse model, 125 islets seeded on scaffolds implanted into the epididymal fat pad restored normoglycemia within an average of 1.95 days and transplantation of only 75 islets required 12.1 days. Increasing the pore size to increase islet-islet interactions did not significantly impact islet function. The porcine model was used to investigate early islet engraftment. Increasing the islet seeding density led to a greater mass of engrafted islets, though the efficiency of islet survival decreased. Transplantation into the porcine omentum provided

*Address Correspondence to: Lonnie D. Shea, Department of Chemical and Biological Engineering, 2145 Sheridan Rd/E136, Evanston, IL 60208, l-shea@northwestern.edu.

Disclosure

The authors confirm that there are no known conflicts of interest associated with this publication and there has been no significant financial support for this work that could have influenced its outcome.

greater islet engraftment than the gastric submucosa. These results demonstrate scaffolds support murine islet transplantation with high efficiency, and feasibility studies in large animals support continued pre-clinical studies with scaffolds as a platform to control the transplant microenvironment.

Introduction

Type 1 diabetes mellitus (T1DM) is a life-long endocrine disorder managed by chronic insulin therapy. Despite advances in insulin types and delivery mechanisms, hypoglycemic events and micro/macro-vascular complications persist [1,2]. Islet transplantation is a promising treatment to ameliorate diabetes and eliminate the need for exogenous insulin therapy. Although current protocols achieve an initial diabetes reversal of over 90%, this rate drops as low as 30% and 10% by 2 and 5 years post-transplantation [3,4]. To achieve diabetes reversal, patients generally receive islets from 2 to 4 donors via hepatic portal infusion. This islet mass represents nearly tenfold more than theoretically needed to maintain normoglycemia [5,6]. Up to 2/3 of transplanted islets die in the first few days post-transplant, and while the remaining islets are sufficient to achieve initial diabetes reversal, hyperglycemia eventually returns as islets are lost [4,5,7].

The current clinical approach of intravascular infusion into a foreign hepatic environment, contributes to islet loss [7,8]. Furthermore, release of islets into the bloodstream initiates a coagulation and complement cascade known as the instant blood-mediated inflammatory reaction (IBMIR) that causes extensive islet damage during the early period following transplantation [7,9]. Although intraportal transplantation encourages physiologic insulin secretion, islets lodged in the hepatic portal vasculature experience a foreign extracellular matrix (ECM), low blood oxygen saturation, and exposure to greater glucose concentrations than are present systemically, as well as elevated levels of ingested toxins, metabolites and pharmaceuticals [10–12]. The development of alternative transplantation sites may enable strategies to modulate the islet microenvironment and thus enhance survival and engraftment in ways not currently possible in the liver [13,14]. Additionally, non-organ sites may enable the retrieval of implants, facilitating the development of alternative islet sources.

To date, a robust and translatable platform that offers a competitive alternative to intraportal infusion has yet to be effectively demonstrated. Extrahepatic sites that avoid the negative influences of intravascular delivery and the hepatic environment have traditionally been limited to organ capsules and surgical pouches. Alternative approaches including kidney capsule, splenic, intramuscular and subcutaneous transplantation have not effectively translated clinically, or failed to demonstrate a significant advantage [13–15]. Biomaterials have shown promise as vehicles for cell transplantation by creating spaces for cell delivery that have the additional potential to modulate the islet microenvironment [16–20]. However, to date, biomaterials research has primarily employed encapsulating strategies, which offered alternatives to immunosuppression, yet are challenged by islet survival, fibrosis and the inability of encapsulated islets to fully revascularize and engraft [15,21].

Alternatively, non-encapsulating, biodegradable microporous scaffolds which provide for integration of the host vasculature, have been successfully employed previously to deliver murine islets in syngeneic models [16,17] and recently in tolerance-inducing allotransplant [19] models. Without isolating islets from the host, these scaffolds physically define an extrahepatic transplant site and provide a platform for future islet-promoting interventions [19,22–25]. In this report, we investigated the architectural modification of the scaffolds to maximize engraftment in a syngeneic mouse model, significantly improving transplantation

efficiency, and demonstrate the translational potential of this platform using a porcine islet allotransplantation model to investigate early islet survival and host compatibility.

Research Design and Methods

2.1. Scaffold fabrication

Scaffolds were fabricated from poly (lactide-co-glycolide) (PLG) microspheres as described previously [16]. Microspheres were formed by homogenizing a 2% or 6% solution of PLG (Lakeshore Biomaterials, Birmingham, AL) in dichloromethane in a solution of 1% polyvinyl alcohol. Washed and lyophilized microspheres were combined in a 1:30 ratio with NaCl particles 250–425 μm or 425–600 μm in diameter. The mixture was pressed in a steel die at 1500 pounds per square inch (psi) and gas-foamed after equilibration to 800 psi CO_2 gas. Salt particles were removed by immersion in water with repeated washing. After drying, scaffolds were rinsed in 70% ethanol and transplant media prior to islet seeding.

2.2. Mouse Islet isolation, scaffold seeding and transplantation

Male C57BL/6 mice (Jackson Laboratories, Bar Harbor ME) 8 to 12 weeks old were used as donors and recipients for transplant studies. Recipients were rendered diabetic 4–5 days pre-transplantation with 220 mg/kg streptozotocin (Sigma-Aldrich, St. Louis, MO) in citric acid buffer injected intraperitoneally. Non-fasting blood glucose was measured using tail blood samples and a OneTouch Basic (Lifescan, Milpitas, CA) glucometer. Recipients were considered diabetic if blood glucose measurements greater than 300 mg/dl were maintained on two consecutive days pre-transplant.

Islets were isolated from healthy donor mice using collagenase digestion as previously described [16]. Isolated islets were hand-counted and seeded on scaffolds using a fine glass pipette. Islet-seeded scaffolds were incubated under a meniscus of media (Hanks buffered salt solution with 5% fetal bovine serum) at 37°C and 5% CO_2 for 30–40 min prior to transplantation. Recipients were anesthetized with an intraperitoneal injection of ketamine (Ketaset®, Fort Dodge, IA) and xylazine (Anased®, Lloyd Labs, IA) The abdomen was shaved, sterile-prepped. A midline incision was made, and the epididymal fat pad (EFP) identified and spread on the abdominal surface. Islet-seeded scaffolds were wrapped in the EFP and returned to the abdominal cavity. The wound was closed in two layers. Mice were given analgesics pre and post-operatively as needed, and monitored for signs of infection or duress. All murine studies were approved by the Northwestern University Animal Care and Use Committees.

2.3. Porcine Islet isolation and transplantation

2.3.1. Islet isolation and quality control—Porcine islets were isolated and cultured as previously described [26,27]. Islet quality control [28,29] revealed an average islet equivalent (IEQ) recovery after 7 day culture of 70±11%. With respect to purity, 95±0% of cells were endocrine cells. The fractional viability measured by the oxygen consumption rate/DNA was 199±60. Islets were seeded on scaffolds similar to murine studies.

2.3.2. Immunosuppression—Pig immunosuppression consisted of CTLA4-Ig (Abatacept, Orencia™; Bristol-Myers Squibb, New York, NY) and sirolimus (Rapamycin, RAPAMUNE ®, Wyeth, Collegeville, PA). CTLA4-Ig was administered intravenously on day 0 and 7. Sirolimus was given mixed with food, an oral loading dose of 2mg/kg on day minus 1 then 1mg/kg, twice daily, starting on day 1 until day 13.

2.3.3. Islet Transplantation—Pigs were fasted overnight but allowed access to water. They were premedicated with Telazol (Wyeth, Fort Dodge, IA, USA) 6 mg/kg

intramuscularly and propofol (20 mg) intravenously. Prophylactic antibiotics, ceftiofur 5mg/kg and gentamicin 3mg/kg, were administered intramuscularly prior to surgery. Anesthesia was induced with isoflurane and oxygen. Pigs were intubated and maintained on 2% isoflurane and 100% oxygen. The abdomen was entered through an upper midline incision and the anterior wall of the stomach was exposed. In two animals, saline was injected into the gastric submucosa (GSM) to create a pocket, then incised and expanded using blunt dissection. Scaffolds seeded with islets were placed into the pocket, with the islet surface in contact with the submucosa. In the other two animals, the greater curvature of the stomach was exposed and islet seeded scaffolds were tacked to the surface using nonabsorbable suture. The omentum (OM) was then folded over the scaffolds, directly in contact with islets, and tacked. The abdominal incision was closed in three layers in a normal fashion.

2.3.4. Postoperative care—The animals received buprenorphine 0.01–0.03mg/kg twice daily for at least 48 hours post operatively. Animals were clinically assessed daily and weighed weekly. Additional postoperative analgesic or antibiotic was given where clinically indicated. All porcine studies were approved by the University of Minnesota Institutional Animal Care and Use Committees.

2.4. Mouse histology

Mice were rendered diabetic and transplanted with 150 syngeneic islets on scaffolds for the purposes of histology (n=4). After fourteen days, mice were infused with a biotinylated tomato lectin (TL, 2mg/ml, Vector Labs, Burlingame, CA) diluted 1:1 with heparin (1,000U/ml), via the femoral vein to label functional, blood-receiving vasculature. After allowing TL to circulate for 8–10 min, the implant-containing EFP was removed, fixed and paraffin-embedded. 5 μm sections were stained with hematoxylin and eosin (H&E), Masson's trichrome (Polyscience, Warrington, PA), or probed with immunohistochemistry as follows: For insulin/lectin double-staining, fluorescein-conjugated goat anti-biotin (1:200, Vector Labs) identified the infused TL, and a guinea pig anti-insulin (1:25, Dako, Carpinteria, CA) followed by Alexa Fluor(AF)-546-conjugated goat anti-rabbit (1:500, Invitrogen, Carlsbad, CA) was used to identify insulin-positive cells with Hoechst (1:2000, Invitrogen) nuclear counterstaining. For insulin and proliferating cell nuclear antigen (PCNA) double-staining, Rabbit anti-PCNA (1:400, Abcam, Cambridge, MA) followed by AF-546 goat anti-rabbit, and the previously-used anti-insulin with an AF-488-conjugated goat anti-rabbit (1:200, Invitrogen) was used to identify insulin-positive cells with Hoechst nuclear counterstaining.

2.5. Porcine Histology

At 14 days post-transplant, all four pigs were euthanized and scaffold-containing implants were retrieved for histology. Samples were snap frozen in −20°C isopentane and embedded in Tissue-Tek O.C.T. (Miles Scientific, Elkhart, IN). Staining was performed on 14 μm cryosections as follows: For insulin area analysis, guinea pig anti-insulin (1:300, Dako) and a biotinylated goat anti-rabbit (1:200) were used with an ABC kit and DAB (Vector Labs) counterstained with hematoxylin. For lectin/insulin double-staining, biotinylated DBA lectin (1:1000, Vector Labs) with an ABC/DAB secondary was used to label vasculature while guinea pig anti-insulin and a biotinylated goat anti-rabbit with an ABC kit and VIP (Vector Labs) was used to identify insulin-positive cells. For Ki67/insulin immunofluorescent double-staining, mouse anti-human Ki67 (1:50, MIB-1, Dako) with an AF-546-conjugated goat anti-mouse secondary was combined with guinea pig anti-insulin and an AF-488 conjugated goat anti-rabbit secondary and counterstained with Hoescht to identify proliferating, insulin-positive cells.

2.6. Quantification and histological analysis

Stained slides were imaged and stitched together using PTGui Pro (New House Internet Services B.V., Rotterdam, The Netherlands) and analyzed with NIH ImageJ (http://rsb.info.nih.gov/ij/). For porcine islet areas, the pixel areas of insulin-positive tissue in serial sections of each implant (≥10 non-adjacent sections/sample, equally distributed across whole sample) were quantified. For vascularization, slides adjacent to those used for insulin were analyzed by counting the lectin-positive pixels within insulin-positive islets using the ratio of pixel areas. The slides for each sample and condition were averaged, compared and normalized. Similarly, to identify proliferation, the number of Ki67-positive nuclei within insulin-positive areas was represented as a proliferating-nuclei-to-islet-area ratio for each slide.

2.7. Statistics

Results are presented as mean ± standard error of the mean (SEM). The student's t-test or one-way analysis of variance with post-hoc Bonferroni's test was used to determine statistical significance as appropriate. Differences in the number of days for diabetes reversal were compared using the Kaplan-Meier survival analysis (Prism Software, GraphPad, CA). A value of probability (p) < 0.05 was considered statistically significant.

Results

3.1. Scaffold architecture impacted islet engraftment in syngeneic mouse model

The impact of scaffold architecture on islet engraftment was examined by manipulating the density and distribution of polymer microspheres. In contrast to previously-reported scaffolds fabricated with microspheres made from a 2% polymer solution [16,17], the scaffolds used herein (Fig 1A) maintained the same microspheres-to-salt mass ratio, but used microspheres fabricated with a 6% solution. These 6% microspheres had a greater density relative to 2%, and thus scaffolds required fewer microspheres to achieve the same polymer mass. This modification was proposed to increase the scaffolds' pore interconnectivity, which could enhance cell infiltration rates. Additionally, by reducing the total amount of materials used, scaffolds were fabricated at 2 mm in height to minimize the overall implant mass. The cell infiltration rate was investigated for scaffolds fabricated from 6% and 2% microspheres. After 14 days, 6% scaffolds were fully infiltrated with host cells, yet 2% scaffolds were not fully infiltrated (Fig 1B).

Islets seeded on the 6% scaffolds and implanted in the EFP of mice reversed streptozotocin-induced diabetes more rapidly than the previous scaffold design. The 2% scaffold was previously reported to require 20.0±7 days for reversal of diabetes with 125 syngeneic islets [17], whereas these modifications resulted in diabetes reversal 1.95±0.68 days post-transplant in all mice (n=19) (Fig 1C). Our results demonstrate that the scaffold architecture and host cell infiltration can impact islet engraftment.

3.2. Syngeneic islets on scaffolds were well-engrafted in mice

Analysis of explant histology indicated that scaffolds were well-tolerated immunologically and completely penetrated by host cells. Macrophages and an occasional multinucleated giant cell were observed at polymer-tissue interfaces, consistent with a mild foreign body response, which importantly, did not lead to fibrotic encapsulation. A dense lymphocytic infiltrate was not observed in the scaffold, islets, or tissue surrounding the implant (Fig 2A), suggesting that a specific, T-cell mediated response was not generated. As seen by immunofluorescent staining, insulin-positive cells maintained an islet-like morphology, without evidence of dissociation or central necrosis (Fig 2B). Islets demonstrated a dense, functional vasculature as visualized by staining for infused TL, which indicates that islets

were able to stimulate extensive angiogenesis (Fig 2C). Islets additionally contained proliferating cells as indicated by PCNA staining, suggesting that turnover and remodeling were occurring within the islets (Fig 2D). These data demonstrate that syngeneic islets on scaffolds were engrafted, densely revascularized and contained proliferating cells within 14 days of transplantation.

3.3. Scaffolds supported minimal mass of islets in mice

We subsequently investigated a reduction in islet number by seeding scaffolds with 75 islets, a 40% reduction compared to our initial studies and previous reports [16,17]. Diabetes was reversed in all mice (n=10), within an average time of 12.1±4.1 days (Fig 3A, 3B). Weight gain was not statistically different than in mice receiving 125 islets (data not shown). Using this minimal islet mass, the role of scaffold architecture was further investigated by increasing the scaffold pore size. Scaffolds were fabricated with 425–600 μm diameter salt particles, an increase from the previously-used 250–425 μm particles. After islet seeding, several islets per pore were observed in 425–600 μm pores, providing for multiple islet-islet interactions, whereas with the 250–425 μm pores, islets were present individually and occasionally in pairs (Fig 3B). Utilizing the large pore scaffolds, diabetes was reversed in all mice within an average of 11.6±4.1 days (n=10). Thus, diabetes reversal and weight gain (data not shown) were not statistically affected by the different pore sizes (Fig 3C). These data suggest that increased direct contact between islets did not significantly impact transplant function.

3.4. Scaffolds supported islet survival and engraftment in a porcine model

The pre-clinical translation of these scaffolds was then investigated by transplanting allogeneic islets into four pigs. The porcine model utilized a significantly larger islet mass and employed immunosuppression to prevent islet rejection. To demonstrate scalability, scaffold diameter was increased to 13 mm, while maintaining the same formulation used previously, and each animal received between 4 and 7 scaffolds. Porcine islets were transplanted on scaffolds (10k IEQ/scaffold) into the GSM or OM of four recipient pigs (n=2 each). The GSM was selected as an attractive, potentially laparoscopically-accessible site with dense vasculature and portal drainage [30]. Similarly, the OM has portal vascular drainage, significant angiogenic and wound-healing capabilities and a promising track record [31–33]. Scaffolds were implanted (Fig 4A) and retrieved 14 days later for investigation of early survival and host compatibility. Gross examination (Fig 4B) of the explanted tissue and histology revealed a minimal inflammatory reaction paralleling the observations in the mouse model. Masson's trichrome staining demonstrated the complete ingrowth of host tissue into the scaffolds without dense lymphocytic infiltration (Fig 4C). Staining for insulin revealed significant areas of islet survival and the maintenance of a clustered islet morphology (Fig 4D). These results indicate that the scaffolds were well-tolerated in the porcine model, and supported significant islet survival after 14 days.

At the OM site, two additional seeding densities (1000 (1k) and 4000 (4k) IEQ/scaffold) were investigated to assess the impact of islet density and transplant site on survival. Islet survival in each condition was analyzed by normalizing to the islet area observed at the lowest (1k) density. Scaffolds seeded with 4k and 10k IEQ had 1.79±0.36 and 6.09±1.02 fold increases in the average islet area. This result represents approximately 45–60% of the expected islet area based on the islet mass transplanted. For the GSM site, scaffolds seeded with 10k IEQ, had islet areas 2.82±0.72 fold higher than the 1k OM, suggesting increased islet loss relative to the OM. These data (Fig 4E, Table 1) demonstrate the impact that transplant site and seeding density had on islet mass.

3.5. Porcine islet vascularization, but not proliferation dependent on seeding density

Revascularization and cell proliferation within islets were also assessed as a function of transplant site and seeding density. Lectin and insulin double-staining (Fig 5A) demonstrated that islets and the scaffold were well-penetrated by multiple host vessels. Analysis revealed that islets at 10k IEQ/scaffold had a significantly lower lectin:insulin area ratio for both transplant sites (GSM: 0.95±0.17 and OM: 1.35±0.25) than islets seeded in the OM site at 4k and 1k IEQ/scaffold (4k: 2.51±0.19 and 1k: 2.21±0.24)($p \leq 0.05$). At 10k IEQ/scaffold, the GSM and OM sites were not significantly different. Proliferation within islets, determined with Ki67 and insulin double-staining, demonstrated multiple proliferating, insulin-positive cells within the islets (Fig 5B). In contrast to revascularization, no significant difference in the Ki67-positive nuclei:insulin area ratio was observed as a function of seeding density or transplant site. Together, these data (Table 2) suggest that seeding density had a greater impact on the revascularization of allogeneic islets than the choice of extrahepatic transplant site. Furthermore, in this model, proliferation was not significantly impacted by seeding density or transplantation site.

Discussion

Intraportal transplantation of healthy islets as a therapy for T1DM is limited by inefficient islet engraftment and compromised long-term survival. These limitations have motivated the development of alternative, extrahepatic transplantation sites. However, one has not yet been demonstrated as sufficiently effective to be applied clinically (reviewed in [13,14]). Many sites are challenged by the islet mass requirement, surgical environment or native vascularity. Biomaterials may facilitate the development of such sites by defining a transplant space, providing a support for islet seeding, and modulating the microenvironment experienced by transplanted islets. With further development, scaffolds may provide opportunities to significantly enhance engraftment though drug, gene or trophic factor delivery, extracellular matrix presentation and cell co-transplantation [17,19,22–25]. The studies herein demonstrate a non-encapsulating, biodegradable scaffold system that is highly effective in the mouse, and its scaling and translation to a large-animal preclinical model.

The scaffold micro-architecture influenced the transplant microenvironment and impacted the engraftment of transplanted islets. In mice, modulating the microspheres' density influenced the rate of host cell infiltration, and by 14 days, the scaffolds were well-infiltrated and supported by host tissue. The islets maintained a healthy morphology, and the architectural modifications significantly improved the rate of diabetes reversal with 125 islets in the mouse model, and enabled diabetes reversal with only 75 islets. This islet mass represents only one-third to one-half of the mass found in a healthy mouse pancreas, and is a substantial reduction relative to our previous reports and the reports of other biomaterials-based delivery systems [16–18,34]. We also investigated the contact between islets as a factor affecting survival via inter-islet signaling. Fabricating scaffolds with a larger pore size increased the number of islets in contact or in close proximity with each other. However, the increased pore size and islet contact did not have a significant impact on diabetes reversal.

Transplanted islets must revascularize and integrate with the host to resume normal physiological functions. Previously avascular islets transplanted on scaffolds were densely revascularized after 14 days, demonstrating that islets recruited significant functional vessel ingrowth. PCNA staining revealed multiple dividing cells within the islets, suggesting the islets are healthy enough to resume physiologic maintenance of the islet structure, which involves beta cell proliferation and turnover. Importantly, the presence of macrophages on the scaffold surfaces yet lack of a fibrotic capsule or dense lymphocytic infiltrate indicated only a mild foreign body response without a specific immunological reaction.

We also demonstrated the transplantation of scaffolds with islets to a large animal, pre-clinical model; which has been one of the major hurdles to the development of extrahepatic islet transplantation platforms. The scaffold diameter was increased to 13 mm, and was found to be compatible with porcine islet allotransplantation model. After GSM or OM implantation, scaffolds and islets appeared intact, with minimal host inflammation. Histology revealed that scaffolds did not generate a fibrotic capsule and were well-infiltrated and supported by host tissue. Allogeneic islets transplanted on the scaffolds maintained a clustered morphology without necrotic centers or lymphocytic infiltrate. Islets appeared histologically similar to the transplants in mice, demonstrating their feasibility as a transplant platform for future pre-clinical studies.

Translation to pre-clinical models involves a large increase in the islet mass requirement and overall implant size, resulting in islet seeding densities that can impact islet survival and engraftment. The islet density created by seeding of 75 murine islets on a scaffold with a 5 mm diameter corresponds to approximately 1k porcine IEQ on a scaffold with a diameter of 13 mm. With the typical curative islet mass delivered to large animals, this density of islets might not be practical due to the resulting number of scaffolds required. To minimize the overall implant size, we investigated three seeding densities (1k, 4k and 10k IEQ) and two transplant locations for their impact on islet survival. The engrafted islet areas measured in histological samples from the OM revealed at higher densities, loss of anticipated islet area based on the seeding density. Thus, although islet survival efficiency declines with increasing seeding density, a six-fold larger surviving mass can still be obtained from each scaffold, suggesting higher densities should be used to reduce the overall implant size in future studies. While the efficiency of seeding appeared to be similar between 4k and 10k IEQ, the highest seeding density negatively impacted islet revascularization. To enhance islet engraftment at high densities, vascularization could be improved by optimizations such as localized trophic factor delivery from scaffolds [23]. The analysis also demonstrated increased survival at the OM relative to the GSM. This enhancement in islet area may be related to the inherent vascularity, wound-healing potential and growth factors present at different anatomical sites.

Conclusions

Herein, we have demonstrated the effectiveness of microporous scaffolds as a platform for extrahepatic islet transplantation in small and large animal models. We determined that scaffold architecture can significantly impact islet survival, and that the system can support diabetes reversal with only 75 islets in the syngeneic murine model. Porcine studies revealed the effective translation to a large animal model, where analysis of early islet survival at two transplant sites and three seeding densities demonstrated decreasing efficiency at higher densities, but the capability to engraft a higher overall islet number. These results will guide the choice of transplant site, scaffold size and number, and islet seeding density in future work while providing opportunities to modulate the transplant microenvironment at extrahepatic sites in ways currently unachievable with intraportal islet infusion.

Acknowledgments

The technical support of Marina Zelivyanskaya and Samantha Holland for histology development is greatly appreciated. Christopher Rives contributed significantly to the development of the scaffold architectural design.

Funding Sources: NIH/NIDDK

References

1. Cryer PE. The barrier of hypoglycemia in diabetes. Diabetes. 2008; 57:3169–76. [PubMed: 19033403]
2. Pambianco G, Costacou T, Ellis D, Becker DJ, Klein R, Orchard TJ. The 30-year natural history of type 1 diabetes complications: The pittsburgh epidemiology of diabetes complications study experience. Diabetes. 2006; 55:1463–9. [PubMed: 16644706]
3. Pattou F, Alejandro R, Barton FB, Hering BJ, Wease S. 2009 update from the collaborative islet transplant registry. Transpl Int. 2009; 22:45–6.
4. Ryan EA, Paty BW, Senior PA, Bigam D, Alfadhli E, Kneteman NM, et al. Five-year follow-up after clinical islet transplantation. Diabetes. 2005; 54:2060–9. [PubMed: 15983207]
5. Emamaullee JA, Shapiro AM. Factors influencing the loss of beta-cell mass in islet transplantation. Cell Transplant. 2007; 16:1–8. [PubMed: 17436849]
6. Berney T, Rudisuhli T, Oberholzer J, Caulfield A, Morel P. Long-term metabolic results after pancreatic resection for severe chronic pancreatitis. Arch Surg. 2000; 135:1106–11. [PubMed: 10982519]
7. Barshes NR, Wyllie S, Goss JA. Inflammation-mediated dysfunction and apoptosis in pancreatic islet transplantation: Implications for intrahepatic grafts. J Leukoc Biol. 2005; 77:587–97. [PubMed: 15728243]
8. Robertson RP. Intrahepatically transplanted islets--strangers in a strange land. J Clin Endocrinol Metab. 2002; 87:5416–7. [PubMed: 12466328]
9. Bennet W, Groth CG, Larsson R, Nilsson B, Korsgren O. Isolated human islets trigger an instant blood mediated inflammatory reaction: Implications for intraportal islet transplantation as a treatment for patients with type 1 diabetes. Ups J Med Sci. 2000; 105:125–33. [PubMed: 11095109]
10. Lee Y, Ravazzola M, Park BH, Bashmakov YK, Orci L, Unger RH. Metabolic mechanisms of failure of intraportally transplanted pancreatic beta-cells in rats: Role of lipotoxicity and prevention by leptin. Diabetes. 2007; 56:2295–301. [PubMed: 17563069]
11. Shapiro AM, Gallant HL, Hao EG, Lakey JR, McCready T, Rajotte RV, et al. The portal immunosuppressive storm: Relevance to islet transplantation? Ther Drug Monit. 2005; 27:35–7. [PubMed: 15665744]
12. Nanji SA, Shapiro AM. Islet transplantation in patients with diabetes mellitus: Choice of immunosuppression. BioDrugs. 2004; 18:315–28. [PubMed: 15377174]
13. Merani S, Toso C, Emamaullee J, Shapiro AM. Optimal implantation site for pancreatic islet transplantation. Br J Surg. 2008; 95:1449–61. [PubMed: 18991254]
14. van der Windt DJ, Echeverri GJ, Ijzermans JNM, Cooper DKC. The choice of anatomical site for islet transplantation. Cell Transplant. 2008; 17:10.
15. Kizilel S, Garfinkel M, Opara E. The bioartificial pancreas: Progress and challenges. Diabetes Technol Ther. 2005; 7:968–85. [PubMed: 16386103]
16. Blomeier H, Zhang X, Rives C, Brissova M, Hughes E, Baker M, et al. Polymer scaffolds as synthetic microenvironments for extrahepatic islet transplantation. Transplantation. 2006; 82:452–59. [PubMed: 16926587]
17. Salvay DM, Rives CB, Zhang X, Chen F, Kaufman DB, Lowe WL Jr, et al. Extracellular matrix protein-coated scaffolds promote the reversal of diabetes after extrahepatic islet transplantation. Transplantation. 2008; 85:1456–64. [PubMed: 18497687]
18. Andrades P, Asiedu C, Rodriguez C, Goodwin KJ, McCarn J, Thomas JM. Subcutaneous pancreatic islet transplantation using fibrin glue as a carrier. Transplant Proc. 2007; 39:191–2. [PubMed: 17275503]
19. Kheradmand T, Wang S, Gibly RF, Zhang X, Holland S, Tasch J, et al. Permanent protection of plg scaffold transplanted allogeneic islet grafts in diabetic mice treated with ecdi-fixed donor splenocyte infusions. Biomaterials. 2011; 32:4517–24. [PubMed: 21458857]
20. Perez-Basterrechea M, Briones RM, Alvarez-Viejo M, Garcia-Perez E, Esteban MM, Garcia V, et al. Plasma-fibroblast gel as scaffold for islet transplantation. Tissue Eng Part A. 2009; 15:569–77. [PubMed: 18694292]

21. Beck J, Angus R, Madsen B, Britt D, Vernon B, Nguyen KT. Islet encapsulation: Strategies to enhance islet cell functions. Tissue Eng. 2007; 13:589–99. [PubMed: 17518605]
22. Aviles MO, Shea LD. Hydrogels to modulate lentivirus delivery in vivo from microporous tissue engineering scaffolds. Drug Deliv Transl Res. 2011
23. Chen RR, Silva EA, Yuen WW, Mooney DJ. Spatio-temporal vegf and pdgf delivery patterns blood vessel formation and maturation. Pharm Res. 2007; 24:258–64. [PubMed: 17191092]
24. Jang J-H, Bengali Z, Houchin TL, Shea LD. Surface adsorption of DNA to tissue engineering scaffolds for efficient gene delivery. J Biomed Mater Res A. 2006; 77:50–8. [PubMed: 16353173]
25. Rives CB, des Rieux A, Zelivyanskaya M, Stock SR, Lowe WL Jr, Shea LD. Layered plg scaffolds for in vivo plasmid delivery. Biomaterials. 2009; 30:394–401. [PubMed: 18929408]
26. Kirchhof N, Shibata S, Wijkstrom M, Kulick DM, Salerno CT, Clemmings SM, et al. Reversal of diabetes in non-immunosuppressed rhesus macaques by intraportal porcine islet xenografts precedes acute cellular rejection. Xenotransplantation. 2004; 11:396–407. [PubMed: 15303976]
27. Brandhorst H, Brandhorst D, Hering BJ, Bretzel RG. Significant progress in porcine islet mass isolation utilizing liberase hi for enzymatic low-temperature pancreas digestion. Transplantation. 1999; 68:355–61. [PubMed: 10459538]
28. Ricordi C, Gray DW, Hering BJ, Kaufman DB, Warnock GL, Kneteman NM, et al. Islet isolation assessment in man and large animals. Acta Diabetol Lat. 1990; 27:185–95. [PubMed: 2075782]
29. Papas KK, Suszynski TM, Colton CK. Islet assessment for transplantation. Curr Opin Organ Transplant. 2009; 14:674–82. [PubMed: 19812494]
30. Echeverri GJ, McGrath K, Bottino R, Hara H, Dons EM, van der Windt DJ, et al. Endoscopic gastric submucosal transplantation of islets (endo-sti): Technique and initial results in diabetic pigs. Am J Transplant. 2009; 9:2485–96. [PubMed: 19775318]
31. Garcia-Gomez I, Goldsmith HS, Angulo J, Prados A, Lopez-Hervas P, Cuevas B, et al. Angiogenic capacity of human omental stem cells. Neurol Res. 2005; 27:807–11. [PubMed: 16354540]
32. Kin T, O'Neil JJ, Pawlick R, Korbutt GS, Shapiro AM, Lakey JR. The use of an approved biodegradable polymer scaffold as a solid support system for improvement of islet engraftment. Artif Organs. 2008; 32:990–3. [PubMed: 19133030]
33. Hefty TR, Kuhr CS, Chong KT, Guinee DG, Wang W, Reems JA, et al. Omental roll-up: A technique for islet engraftment in a large animal model. J Surg Res. 2010; 161:134–8. [PubMed: 19394649]
34. Dufour JM, Rajotte RV, Zimmerman M, Rezania A, Kin T, Dixon DE, et al. Development of an ectopic site for islet transplantation, using biodegradable scaffolds. Tissue Eng. 2005; 11:1323–31. [PubMed: 16259588]

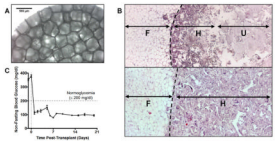

Figure 1. Scaffold design impacts islet engraftment in syngeneic mouse model

(A) Light microscopy of scaffold architecture prior to islet seeding and transplant. Pores are 250–425 μm in diameter. (B) H&E of cellular infiltration of scaffolds 14 days post-transplant. Scaffold made from 2% PLG microspheres (top) is poorly penetrated by host tissue, while scaffold made with 6% PLG microspheres (bottom) is completely infiltrated. Dashed line represents scaffold margin, (F)=Epididymal fat, (H)=Scaffold infiltrated with host tissue, (U)=Uninfiltrated scaffold. (C) Average blood glucose of mice receiving 125 islets on scaffolds (n=19). Kaplan Meier analysis of diabetes reversal with 125 islets can be seen in Figure 3B.

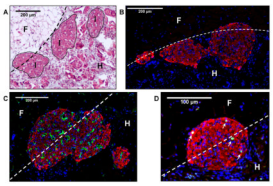

Figure 2. Syngeneic mouse islets on scaffolds are engrafted, revascularized and have proliferating cells

(A) Masson's trichrome image of syngeneic mouse islets transplanted on scaffolds after 14 days. Note the host tissue infiltration and lack of fibrotic capsule or lymphocytic infiltrate. (B) Immunofluorescent staining of islet morphology demonstrates maintenance of islet morphology 14 days post-transplant. Red=insulin, Blue=nuclei. (C) Immunofluorescent staining of dense functional vasculature inside islet. Avascular at transplant, after 14 days, islets had a high vascular density featuring numerous vessels. Red=insulin, Green=lectin-positive vasculature, Blue=nuclei. (D) Immunofluorescent staining of proliferating nuclei inside islet. White arrows indicate proliferating cells within the islet 14 days post-transplant. Red=Insulin, Green=PCNA-positive nuclei, Blue=nuclei. Dashed line=scaffold margin, (I) Islets, (F) Epididymal Fat, (H) Scaffold infiltrated with host tissue.

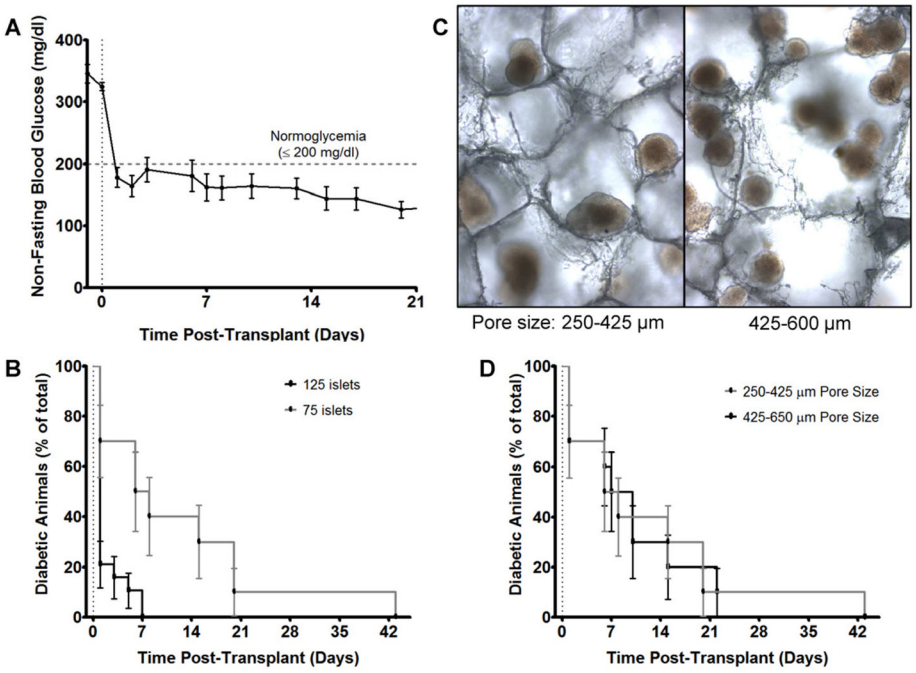

Figure 3. Scaffold support diabetes reversal with 75 syngeneic islets at IP fat pad site in mice

(A) Average blood glucose of mice receiving 75 islets on scaffolds and (B) Kaplan Meier analysis of diabetes reversal. 75 islets reversed diabetes in all mice (n=10) with an average time to euglycemia of 12.1±4.1 days. 125 islets (n=19) reversed diabetes in all mice in an average of 1.95±0.68 days. (C) After islet seeding, scaffolds with 250–425 μm pores had islets individually or occasionally in pairs within pores, whereas scaffolds with larger pores had several islets per pore, providing for multiple islet-islet interactions. (D) Kaplan Meier analysis of diabetes reversal in mice receiving 75 islets on scaffolds with different pore sizes (n=10 each). No statistical difference was observed. Polymer scaffolds were formed with 6% PLG microspheres.

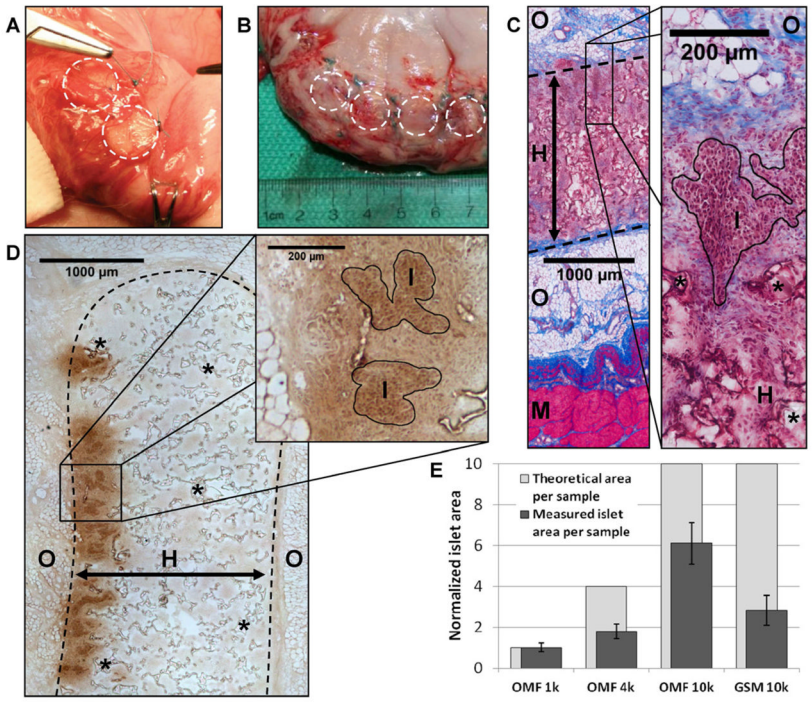

Figure 4. Scaffolds support islet survival in a porcine allogeneic model

(A) Image of scaffolds being implanted in OM. Scaffolds were tacked to the stomach surface, and the OM was pulled over the islet-containing scaffold surfaces. Dashed circles indicate scaffold margins. **(B)** Image of OM scaffolds explanted at 14 days. No significant inflammation is apparent. **(C)** Masson's trichrome staining of scaffold implant demonstrates complete host infiltration after 14 days and a minimal inflammatory reaction. **(D)** Insulin staining (brown) reveals significant islet survival and maintenance of islet morphology. **(E)** Analysis of insulin-positive islet areas in serial sections reveals differences in surviving islet mass at multiple seeding densities (10k, 4k, 1k IEQ) and implantation sites (OM and GSM). Plotted in dark gray are the observed islet areas for the different conditions and in light gray, the theoretical area expected, normalized to the 1k OM site. (I)=islets, (S)=scaffold, (H)=host tissue infiltration of scaffold, (O)=omentum, (M)=muscularis of stomach wall, (*)=remaining scaffold polymer, Dashed line indicates scaffold margins.

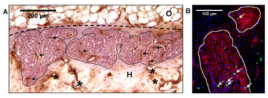

Figure 5. Porcine islet vascularization, but not proliferation, is dependent on seeding density

(A) Insulin staining by VIP (purple) and vascular staining with DAB (brown) reveals significant vascularization of engrafted islets. Dashed line represents scaffold margin, (O)=Omental fat, (H)=Scaffold infiltrated by host tissue, Black arrows indicate representative vascular structures, (*) indicate scaffold polymer **(B)** Immunofluorescent staining of proliferating nuclei inside porcine islet. White border demarcates insulin-positive areas (islets). White arrows indicate proliferating cells within islet. Red=Insulin, Green=Ki67-positive nuclei, Blue=nuclei.

Table 1

Islet area analysis of seeding density and transplant site in porcine model

Transplant site	Seeding density	Samples (n)	Slides Quantified	Islet area per sample (normalized mean±sem)	Theoretical area per sample	Area % less than expected
OMF	1k	2	27	1.00 ± 0.21	1.0	0.0%
OMF	4k	2	26	1.79 ± 0.36	4.0	55.3%
OMF	10k	2	20	6.09 ± 1.02	10.0	39.1%
GSM	10k	2	23	2.82 ± 0.72	10.0	71.8%

Table 2

Analysis of transplant site and seeding density in porcine islet transplants on scaffolds.

		Lectin/islet area			Ki67(+) nuclei/islet area		
Transplant Site	**Seeding Density**	**Slides (n)**	**Mean**	**SEM**	**Slides (n)**	**Mean**	**SEM**
OM	1k	16	2.21	0.24	9	2.57	0.19
OM	4k	10	2.51	0.19	6	3.22	0.59
OM	10k	20	1.35	0.25	12	2.29	0.23
GSM	10k	10	0.95	0.17	7	2.12	0.15

Normalized lectin-positive/insulin-positive areas and Ki67-positive nuclei/insulin-positive areas were calculated. Lectin density was higher ($p<0.05$) for islets seeded at 1k and 4k in the OMF than at 10k in the OMF or GSM. No significant difference in the number of Ki67-positive nuclei/insulin-positive area between conditions was observed.